Research Article

Journal of MASS SPECTROMETRY

Received: 28 July 2011 Revised: 22 September 2011 Accepted: 23 September 2011 Published online in Wiley Online Library

(wileyonlinelibrary.com) DOI 10.1002/jms.2000

Reflectron MALDI TOF and MALDI TOF/TOF mass spectrometry reveal novel structural details of native lipooligosaccharides

Luisa Sturiale,[a] Angelo Palmigiano,[a] Alba Silipo,[b] Yuriy A. Knirel,[c] Andrei P. Anisimov,[d] Rosa Lanzetta,[b] Michelangelo Parrilli,[b] Antonio Molinaro[b] and Domenico Garozzo[a]*

Lipooligosaccharides (LOS) are powerful Gram-negative glycolipids that evade the immune system and invade host animal and vegetal cells. The structural elucidation of LOS is pivotal to understanding the mechanisms of infection at the molecular level. The amphiphilic nature of LOS has been the main obstacle for structural analysis by matrix-assisted laser desorption/ionization (MALDI) mass spectrometry (MS). Our approach has resolved this important issue and has permitted us to obtain reflectron MALDI mass spectra of LOS to reveal the fine chemical structure with minimal structural variations. The high-quality MALDI mass spectra show LOS species characteristic of molecular ions and defined fragments due to decay in the ion source. The *in-source* decay yields B-type ions, which correspond to core oligosaccharide(s), and Y-type ions, which are related to lipid A unit(s). MALDI tandem time-of-flight (TOF/TOF) MS of lipid A allowed for the elucidation of its structure directly from purified intact LOS without the need for any chemical manipulations. These findings constitute a significant advancement in the analysis of such an important biomolecule by MALDI MS. Copyright © 2011 John Wiley & Sons, Ltd.

Supporting information may be found in the online version of this article.

Keywords: lipooligosaccharides; lipid A; MALDI TOF; tandem MS; TOF/TOF

INTRODUCTION

Lipopolysaccharides (LPS) are the major component of the outer membrane of Gram-negative bacteria.[1,2] LPS endotoxins are recognized as a key factor in bacterial survival and functionality in all aspects of environment–bacterium interactions, such as recognition, adhesion, colonization, virulence in the case of pathogenic bacteria, symbiosis, tolerance for commensal bacteria and adaptation of extremophile species to their external environment. From a chemical point of view, LPS are amphiphilic and amphiphatic molecules that consist of a hydrophilic carbohydrate portion (subdivided into a core oligosaccharide and an O-polysaccharide chain, O-PS) covalently linked to a hydrophobic lipid A portion, which anchors the whole structure to the outer leaflet of the Gram-negative outer membrane. In some bacteria, the O-PS chain is absent because of genetic mutations, or as a characteristic of the bacterial strain.[2] These types of LPS are designated rough-type (R-type LPS) or lipooligosaccharides (LOS). Certain bacteria express, both within and between strains, LOS that comprise a heterogeneous mixture of molecules due to the structural variability of both lipid A and core oligosaccharide.[2]

Currently, matrix-assisted laser desorption/ionization (MALDI) mass spectrometry (MS) is successfully used in a wide range of advanced analytical applications, including proteomics,[3] glycomics[4] and MS imaging.[5] Despite the continuous development of this technique, intact LOS have resisted structural MALDI analysis because of their amphiphilic nature.[6,7] Molecular mass (MM) measurements are not straightforward for these species due to their strong tendency to form aggregates and intermolecular negative-charge cross links (due to phosphates, pyrophosphates and uronic acids) by divalent cations. Therefore, MALDI analyses have usually been performed separately on lipid A and core oligosaccharide components obtained after acidic hydrolysis and subsequent Bligh–Dyer extraction[1,2] or on *O*-deacylated LOS.[8,9] Furthermore, alternative MS techniques have been developed for LPS analysis.[10,11]

A few years ago, we presented a robust sample preparation method for MALDI analysis of intact LOS[12] using a novel sample-matrix preparation process that allowed us to accomplish routine MALDI analysis of these molecules in their native state.[13] The importance of the sample preparation procedure and matrix choice that allows for proper matrix-to-sample co-crystallization was considered critical at the beginning of the MALDI MS era.

* *Correspondence to: Domenico Garozzo, CNR Istituto per la Chimica e la Tecnologia dei Polimeri, Via P. Gaifami 18, 95126 Catania, Italy. E-mail domenico.garozzo@cnr.it*

a *CNR Istituto per la Chimica e la Tecnologia dei Polimeri, Via P. Gaifami 18, 95126 Catania, Italy*

b *Dipartimento di Chimica Organica e Biochimica, Università degli Studi di Napoli Federico II, Via Cintia 4, I-80126 Napoli, Italy*

c *N. D. Zelinsky Institute of Organic Chemistry, Russian Academy of Sciences, 119991 Moscow, Russia*

d *State Research Center for Applied Microbiology and Biotechnology, 142279 Obolensk, Moscow Region, Russia*

However, after the introduction of the delayed extraction technique and success of the dried-drop preparation method, the value of skilled sample preparations has been increasingly underestimated. The classic dried-drop method fails when the sample tends to aggregate because MM and polydispersity significantly increase, promoting matrix-sample separation into two distinct phases and preventing co-crystallization.[14] Our strategy is the result of a combination of widely known MALDI sample preparation procedures aiming to place the appropriate matrix and LOS molecules into close contact. Each preparation step plays a specific role: (i) dissolving LOS samples in a chelating ethylenediaminetetraacetic acid (EDTA) solution avoids aggregation due to the presence of divalent cations; (ii) mixing a few microliters of this EDTA solution with a small quantity of cation-exchange resin converts phosphates and uronic salts into their acidic forms; (iii) spotting the final compound directly onto the MALDI plate in a matrix thin layer, composed of 2',4',6'-trihydroxyacetophenone monohydrate (THAP) and nitrocellulose, captures salts and other impurities and also provides a non-conductive surface for LOS desorption/ionization.

Spectra obtained by such a method[15–25] are rich in information because the mass spectra show both sets of quasi-molecular ions and well-defined fragments due to in-source decay that yields B-type ions corresponding to the core oligosaccharide(s) and Y-type ions related to lipid A unit(s) (Domon and Costello nomenclature).[26] This fragmentation resembles the typical LPS workup, which consists of mild acidic hydrolysis that splits lipid A from the rest of the saccharide backbone.

The poor stability of LOS quasi-molecular ions is an evident advantage to assign a structure to whole molecule components but represents a distinct disadvantage, because only low-resolution spectra in linear mode could be acquired, whereas the acquisition of high accuracy MALDI mass spectra of unstable molecules in the reflector mode requires stable ions.

Here, we present an improvement in the MALDI MS strategy based on the optimization of the sample-matrix preparation procedure, which includes the hydrophobic coating of the MALDI plate. This method enabled us to obtain reflectron MALDI mass spectra of intact LOS, which yielded accurate MMs for the LOS and its constituents, and MS/MS spectra for structural elucidation of the lipid A moiety.

To test the capabilities of the method, we applied this approach for structural profiling of some widely studied R-type LPS that were extracted from two mutant strains of *Burkholderia cenocepacia* K56-2 and *Shigella flexneri* M90T and from *Yersinia pestis*.

EXPERIMENTAL SECTION

LOS were extracted and purified from dried cells of the respective bacteria following previously described methods.[12,27]

Sample preparation

Approximately 1 mg of lyophilized LOS was added to 150 μL of a 5 mM EDTA solution in methanol/water (1:1 vol/vol). To promote disaggregation, the sample suspension was mixed by vortexing and was placed in an ultrasonic bath for 10 min. Because the presence of contaminating cationic salts can disturb the solubility and efficiency of the desorption/ionization, rapid desalting has to be performed: a small quantity (5–10 μL) of Dowex 50WX8-200 cation-exchange resin was first converted to the ammonium form by repeated washes with water, followed by a wash with a 5% NH_4OH solution, and the resin was placed on top of a small piece of Parafilm®. The excess fluid was removed using a digital pipette and was replaced with the same volume of the sample dispersion. Finally, the sample solution (0.5 μL), along with the same volume of 20 mM dibasic ammonium citrate, was deposited on the matrix thin layer that had been prepared on the MALDI plate. An excess of ammonium ions and their replacement as counter-ions on the acidic sites was essential to produce a volatile species that undergoes proton transfer upon ionization.

Satisfactory spectra were also obtained with a smaller amount of starting material (up to 5–10 μg) to get sample concentration of about 0.03–0.06 μg/μL. This quantity is higher than we actually expect in the final spotted solution after the cleanup step. MS and MS/MS analysis usually include about 20 experiments that need two to three spots per sample.

Matrix preparation

THAP (200 mg) was dissolved in 1 mL of methanol and mixed in a 4:1 ratio (vol/vol) with a solution of 15 mg/mL of nitrocellulose (trans-blot membrane, BioRad) in acetone/propan-2-ol (1:1 vol/vol). These solutions must be freshly prepared daily before use. After the 0.5 μL of the final matrix solution was spotted onto a stainless steel MALDI plate, rapid solvent evaporation resulted in a finely dispersed homogeneous matrix layer as a microcrystalline surface for sample deposition. To avoid spreading the matrix spot over a broad area, the cleaned MALDI plate was treated with commercially available POL metal polishing paste (SPI Supplies), which provides a hydrophobic coating of the whole plate surface. This procedure enhanced the quality of the spectra obtained.

Mass spectrometric analysis

This study used a 4800 Proteomic Analyzer (Applied Biosystems), a MALDI time-of-flight (TOF/TOF) instrument equipped with a Nd:YAG laser at a wavelength of 355 nm with $<$500-ps pulse and 200-Hz firing rate. External calibration was performed using an Applied Biosystems calibration mixture in reflectron mode, or angiotensin in MS/MS mode. Mass accuracy was about 50 ppm. All measurements were performed in negative polarity. Approximately, 2000 laser shots were accumulated for each spectrum in the MS experiments; 4000 to 6000 shots were summed for the MS/MS data acquisitions. The tandem mass spectra reported in this study were acquired without collision gas. A series of MALDI TOF/TOF experiments were also performed with helium, argon, xenon or air as collision gas, and the resulting fragmentation spectra were compared with those obtained without collision-induced dissociation (CID); no significant differences were observed in all the observed cases in the mass range above *m/z* 200. Below this mass, product ions corresponding to the phosphate fragments at *m/z* 79 and 97 were much more abundant in the CID spectra regardless of the collision gas.

RESULTS

Figure 1(a) shows the reflectron MALDI mass spectrum of the LOS from the *wabR* mutant of *Burkholderia cenocepacia* (*B. cenocepacia*) strain K56-2.[28] The mass spectrum shows LOS quasi-molecular ions $(M\text{-}H)^-$ in the higher mass region. At lower masses, peaks corresponding to core oligosaccharide

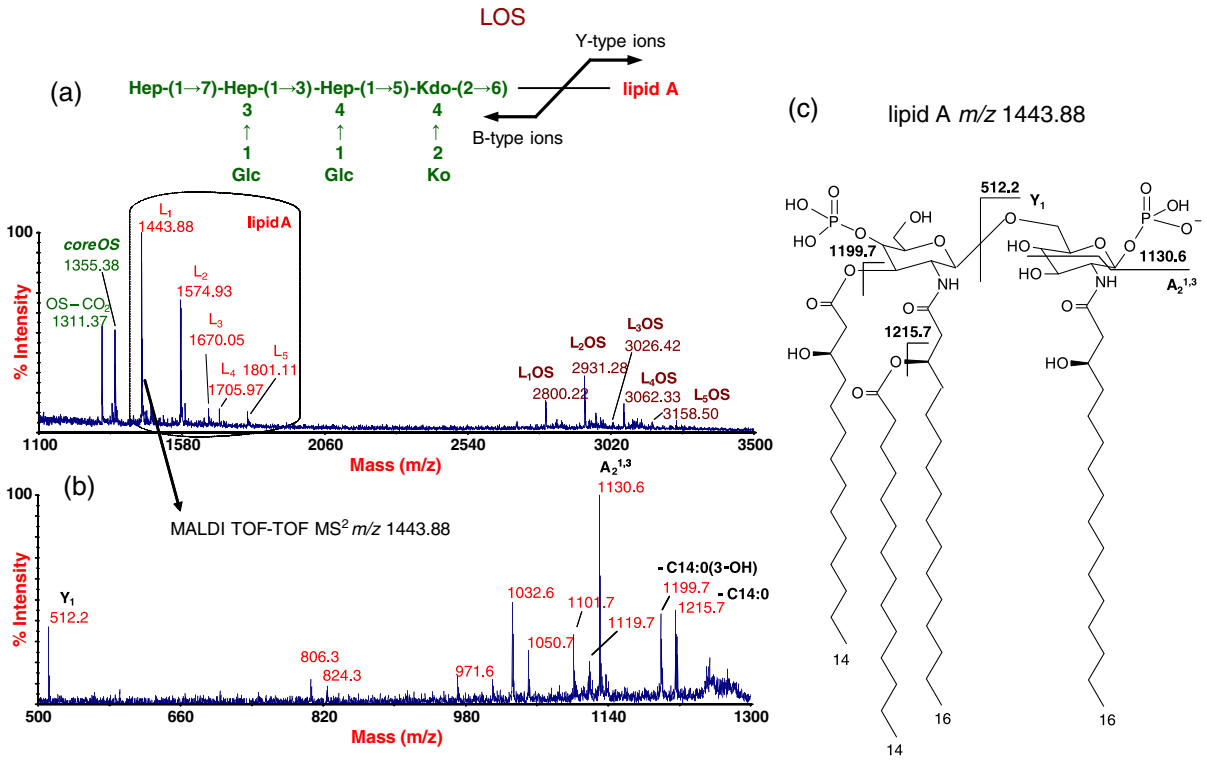

Figure 1. Structural investigation of LOS from *B. cenocepacia* strain K56-2 (*wabR* mutant) by reflectron MALDI TOF MS and MALDI TOF/TOF MS. (a) Negative-ion MALDI TOF mass spectrum of native LOS. (b) Negative-ion MALDI TOF/TOF spectrum of lipid A at *m/z* 1443.88 (L_1). Major fragment at *m/z* 1345.8, originated from the β-elimination of phosphoric acid ($-H_3PO_4$), was not included. (c) Structure of L_1 species and its main MS/MS fragmentations.

and lipid A species (L_1 to L_5) that originate from the in-source fragmentation described above are observed. This mass spectrum was acquired at a resolution of approximately 15,000 for all the species with mass accuracy better than 75 ppm. The reflectron spectra are essential to define details of typical LOS microheterogeneity, including the possible presence of unsaturated fatty acids and controversial structures that cannot be assigned in a low-resolution mass spectrum. B-Type ions that are characteristic of the core oligosaccharides were found at *m/z* 1355.38 and *m/z* 1311.37 (loss of a neutral CO_2 molecule from the 3-deoxy-D-manno-oct-2-ulosonic acid, Kdo), while Y-type ions, which correspond to lipid A species (from L_1 to L_5), were all contained in the inset. L_1 (*m/z* 1443.88) matched with the tetra-acylated lipid A reported in Fig. 1(c), L_2 (*m/z* 1574.93) and L_4 (*m/z* 1705.97) shared the same L_1 basic structure plus one and two 4-aminoarabinose (Ara4N) units, respectively. L_3 (*m/z* 1670.05) corresponded to a penta-acylated lipid A with an additional 3-hydroxymyristic acid [C14:0(3-OH)] in an ester linkage at the C3 position of the proximal glucosamine residue (GlcN I). L_5 (*m/z* 1801.11) fitted the same penta-acylated lipid A bearing one Ara4N residue. Both B- and Y-type ions were generated from the fragmentation (β-elimination) of the glycosidic bond between Kdo and lipid A unit (linked at the C6 position of the distal glucosamine, GlcN II). Peaks corresponding to LOS quasi-molecular ions were present in the mass range between *m/z* 2600 and 3200.

We also extracted the MALDI TOF/TOF mass spectra for the main LOS ions at *m/z* 2800.22, *m/z* 2931.28 and *m/z* 3062.33 (Fig. 2). All three spectra shared the same B-type ion at *m/z* 1355.3, which matched with the identical core oligosaccharide, and showed different Y-type ions related to their respective lipid A counterpart. At first glance, these analyses may appear redundant; however, they provided crucial information because each spectrum contained ion fragments that corresponded to the core oligosaccharide and to its reciprocal lipid A counterpart. This redundancy eliminated the ambiguity concerning the LOS-glycoform and lipid A moiety where they originated. L_1OS (Fig. 2(a)) dissociated and yielded the lipid A component L_1 at *m/z* 1443.8, and L_2OS (Fig. 2(b)) yielded the component L_2 at *m/z* 1574.9, differing from L_1 by the presence of one Ara4N residue. This last species underwent the neutral loss of the labile Ara4N (−131.1 u (unified atomic mass unit)), which gave the ion at *m/z* 1443.8. L_4OS (Fig. 2(c)) dissociated and yielded the lipid A component L_4 at *m/z* 1705.9, which contained two Ara4N units. This fragment easily lost one (peak at *m/z* 1574.9) or both (peak at *m/z* 1443.8) of the Ara4N residues.

To obtain the fine-structure characterization of the lipid A components, the MS/MS spectra of the related (fragment) ions were collected. The MALDI TOF/TOF mass spectrum of the tetra-acylated lipid A moiety (L_1) at *m/z* 1443.88 is reported in Fig. 1(b). Conceptually, it is a MS^3 spectrum obtained with a MS/MS instrument (also reported for *O*-deacylated LOS)[29], as this parent ion is a Y-type fragment originated from the prompt in-source decay of the LOS quasi-molecular ion at *m/z* 2800.22. Peaks observed in this MS/MS spectrum result from fragmentations that occurred in the MALDI TOF/TOF mass spectrometer collision chamber by impact with inert gases or by metastable decay. The main fragmentations are indicated in Fig. 1(c): the peak at *m/z* 1215.7 corresponded to the loss of the secondary myristic acid (C14:0), the peak at *m/z* 1199.7 derived from loss of the primary ester-linked C14:0(3-OH), the peak at *m/z* 1130.6 was related to the cross-ring fragmentation $A_2^{1,3}$ and the peak at

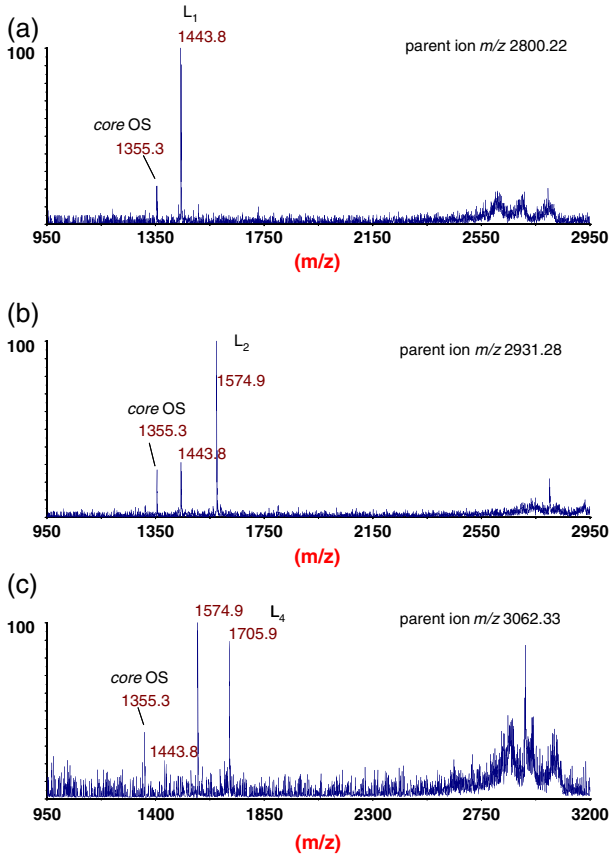

Figure 2. Negative-ion MALDI TOF/TOF analysis of the three major LOS glycoforms from *B. cenocepacia* strain K56-2 (*wabR* mutant): (a) L_1OS at *m/z* 2800.22. (b) L_2OS at *m/z* 2391.28, and (c) L_4OS at *m/z* 3062.33. The broad assembly of not well-resolved peaks is due to metastable transitions and phosphate groups losses.

Table 1. Complete list of the observed MS^2 ions from L_1 at *m/z* 1443.88

Observed ions (*m/z*)	MS/MS assignments
1345.8	$[M - H_3PO_4 - H]^-$
1215.7	$[M - C14:0 - H]^-$
1199.7	$[M - C14:0(3\text{-}OH) - H]^-$
1130.6	$A_2^{1,3}$
1119.7	$[M - C14:0(3\text{-}OH) - HPO_3 - H]^-$
1101.7	$[M - C14:0(3\text{-}OH) - H_3PO_4 - H]^-$
1050.7	$A_2^{1,3} - HPO_3$
1032.6	$A_2^{1,3} - H_3PO_4$
971.6	$[M - C14:0 - C14:0(3OH) - H]^-$
824.3	$A_2^{1,3}$– C14:0(3-OH) – HPO_3
806.3	$A_2^{1,3}$– C14:0(3-OH) – H_3PO_4
512.2	Y_1

m/z 512.2 corresponded to the Y_1 fragment resulting from the cleavage of the glycosidic linkage. The complete list of all the peaks assigned in Fig. 1(b), including multiple fragmentations, is reported in Table 1. The absence of a peak originating from the loss of a whole *O*-acyloxyacyl group, which is composed of C14:0(3-OH) linked to a C14:0 (– 454 u), indicates that the secondary C14:0 fatty acid is present as an *N*-acyloxacyl group.

Fragmentation of lipid A formed by in-source decay follow the same defined rules as lipid A obtained by acidic hydrolysis and permitted us to distinguish fatty acid positions:[30–35] 1) intense ions that originate from fatty acid losses due to the rupture of the ester linkage on each glucosamine (GlcN) residue are present; 2) no loss of amide-linked fatty acid occurs; 3) intense ions corresponding to the Y-type fragment of GlcN I are always observed. By these three guidelines, the complete structure of the lipid A unit can be drawn. Discrimination between O- and N-linked fatty acids was straightforward, due to the higher strength of the amide linkage with respect to the ester bonds. Secondary fatty acids were readily assigned, because they can be lost either as an *O*-acyl secondary substituent or as an *O*-acyloxyacyl group. Based on these observations, differences in the fragmentation pattern enabled also to discriminate between secondary acyl groups on ester-linked and amide-linked fatty acids. Finally, the glycoside bond cleavage allowed for the assignment of fatty acid positions on both reducing and non-reducing GlcN residues. This MS/MS approach allowed for direct LOS structural studies without any chemical manipulation, thus avoiding losses of labile groups. The lipid A structure at *m/z* 1443.88 from the LOS *wabR* mutant of *B. cenocepacia* strain K56-2 was inferred from the MALDI tandem MS method described above (Fig. 1(c)). The fatty acid distribution was slightly dissimilar from that reported for other strains that belong to the *Burkholderia cenocepacia* species (21) as the primary C14:0(OH) fatty acid was here unequivocally located at the O-3 GlcN II position as opposed to the O-3 GlcN I. This novel conclusion is based on the presence of two key fragments found in the MS/MS spectrum shown in Fig. 1(b). The first fragment at *m/z* 512.2 matches with the mono-acylated Y_1 ion, and the other fragment at *m/z* 1130.6 corresponds to the $A_2^{1,3}$ ion, which originated from a ring cleavage promoted by the free OH at the C3 position of the reducing GlcN.

The MS/MS spectrum of the lipid A glycoform at *m/z* 1574.93 (L_2), which represents the tetra-acylated species L_1 (*m/z* 1443.88) plus one Ara4N residue, was also obtained (Supporting information Fig. S1). Observation of the Y_1 ion at mass 643.3 indicated that this glycosidic unit, when present, is always linked to the GlcN I phosphate group. A second Ara4N was even more rare (lower peak L_4 at *m/z* 1705.97 in Fig. 1(a)) and was connected to the GlcN II phosphate, as demonstrated by the same Y_1 peak found in the MS/MS spectrum of L_4 (data not shown).

The potential and versatility of the analytical method was further shown by the study of LOS from the *Shigella flexneri* M90T Δ*galU* mutant.[36] The reflectron MALDI mass spectrum from this species (Fig. 3) showed a plethora of different LOS glycoforms. This spectrum is subdivided into three distinct mass ranges. In the low *m/z* region (Fig. 3(a)), peaks that corresponded to different glycoforms of core oligosaccharide (OS at *m/z* 1026.17, OS1 at *m/z* 903.17 and OS2 at *m/z* 823.21) were present along with peaks due to the neutral loss of CO_2 from Kdo. The middle mass region (Fig. 3(b)) contained lipid A isoforms with the major component being the hexa-acylated lipid A at *m/z* 1796.16. Minor peaks were attributed to a penta-acylated lipid A (*m/z* 1569.98) that lacked the primary 3-hydroxymyristic acid and to a tetra-acylated lipid A (*m/z* 1359.79) that lacked the secondary myristic acid. In the high mass region (Fig. 3(c)), LOS quasi-molecular ions, mainly composed from the most abundant hexa-acylated lipid A, were identified. Fig. 3 also shows the whole LOS structure with the non-stoichiometrically linked moieties outlined in red.

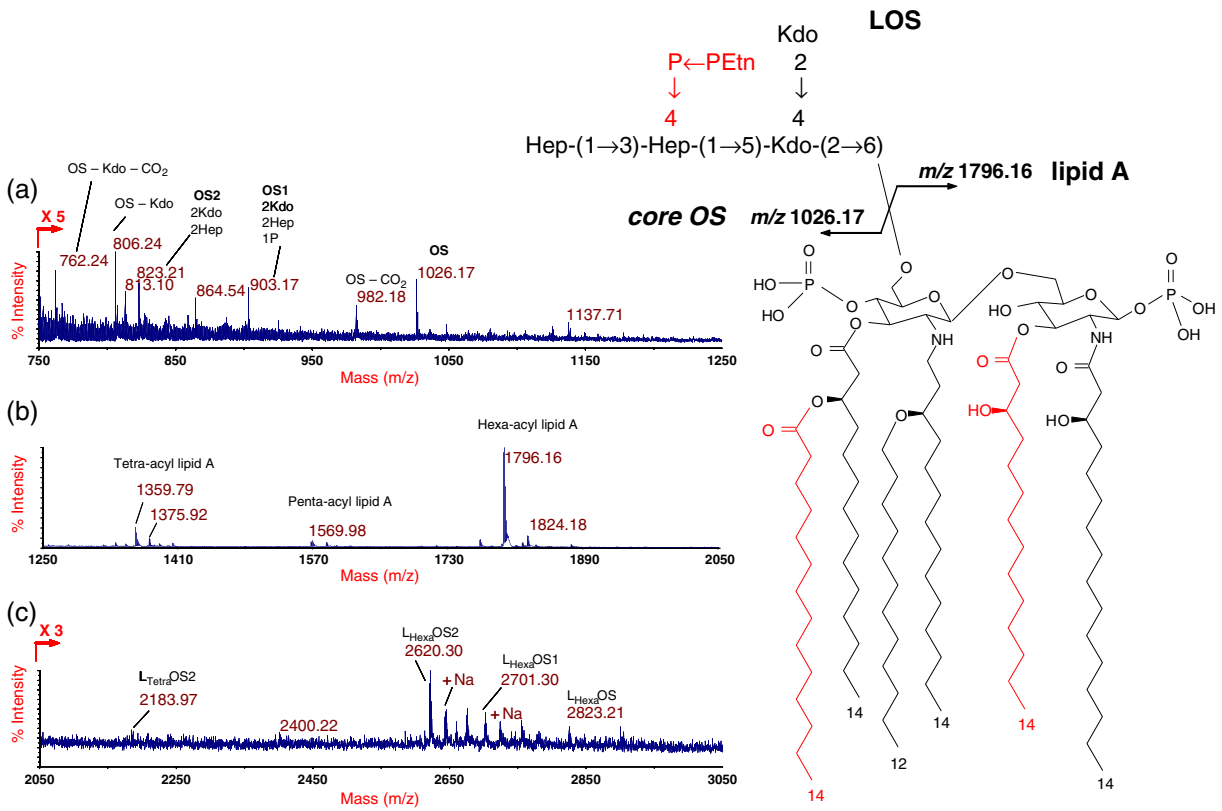

Figure 3. Reflectron MALDI TOF analysis of LOS from *Shigella flexneri* M90T *ΔgalU*. (a) Low mass region. (b) Middle mass region. (c) High mass region. In the figure is also sketched the whole LOS structure with the non-stoichiometrically linked moieties drawn in red.

The tandem mass spectrum of a selected LOS at *m/z* 2823.21 (Fig. 4(a)) revealed the MM of the lipid A and core OS components. The MALDI TOF/TOF mass spectrum of the principal lipid A species (at *m/z* 1796.16) is reported in Fig. 4(b) along with the fragmentation pattern. Peaks corresponding to single fragmentations were present at *m/z* 1698.2 (loss of phosphoric acid), *m/z* 1596.0 (loss of lauric acid), *m/z* 1568.0 (loss of myristic acid), *m/z* 1552.0 (loss of the 3-hydroxymyristic acid linked to the reducing GlcN), *m/z* 1341.8 (loss of the whole *O*-acyloxyacyl group composed of myristic acid linked to 3-hydroxymyristic acid) and *m/z* 710.3 (Y_1 fragment). Ions arising from two or more dissociations were also present and are assigned in the spectrum. These data, along with fatty acid chemical analysis, revealed the structure of the lipid A moiety as previously discussed.

Finally, the MALDI TOF/TOF spectrum of the OS peak at *m/z* 1026.17 is also reported (Fig. 4(c)). The base-peak at *m/z* 806.4 originated from the terminal Kdo loss. Peaks at *m/z* 683.4 and 665.4 indicated a further loss of phosphoethanolamine. The peak at *m/z* 191.0 corresponded to the B_1 ion. These peaks provided some information about the oligosaccharide sequence: one Kdo and one heptose residue were present in terminal positions; therefore, the pyrophosphoethanolamine group must be linked to the second heptose.

The acquisition of reflectron MALDI mass spectra has been demonstrated to be important in the structural analysis of LPS from *Yersinia pestis*. The MALDI mass spectrum in reflectron mode of the R-type LPS from *Y. pestis* P1680 grown at 37 °C (Fig. 5) contained, besides the LPS quasi-molecular ions in the range between *m/z* 1800 and 3000, also Y fragments at *m/z* 1403.81, 1534.83 and 1665.84 that corresponded to the tetra-acylated lipid A species (L_T) bearing none, one or two Ara4N residues, respectively. A less intense peak that corresponded to the core OS was present at *m/z* 1177.34. Focusing on this ion, an additional peak at *m/z* 1177.65 corresponding to a tri-acylated lipid A isoform has been revealed. This last isoform had been previously observed in *Y. pestis* strain Yreka.[11,37] As shown in the figure inset, the instrumental resolution was sufficient to permit discrimination between these two species. The MALDI TOF/TOF mass spectrum of the ion at *m/z* 1177.65 also demonstrated that this lipid A contained three hydroxymyristic acids at C2, C2' and C3' positions (data not shown).

To further substantiate the efficacy of the sample preparation procedure reported here, we also obtained reflectron MALDI mass spectra of LPS from *Y. pestis* KM218 grown at 6 °C along with the MS/MS analysis of its main lipid A component at *m/z* 1822.10 (Supporting information Fig. S2 and Fig. S3). Our results were found to be in good agreement with those obtained by high resolution electrospray Fourier transform ion cyclotron resonance (ESI FTICR), which demonstrated a temperature-dependent variation of *Y. pestis* LPS structures.[38,39] ESI FTICR yields higher resolution that will increase the ability to resolve overlapping peaks and to separate and identify glycolipids species with mass differences of only 0.036 u.[40]

CONCLUSIONS

The optimized sample preparation method presented here provides resolved and reproducible MALDI mass spectra of native LOS and MS/MS of its components lipid A and core OS. These findings present new avenues for LPS endotoxin structural analysis. The MALDI TOF experiment can be successfully adopted and

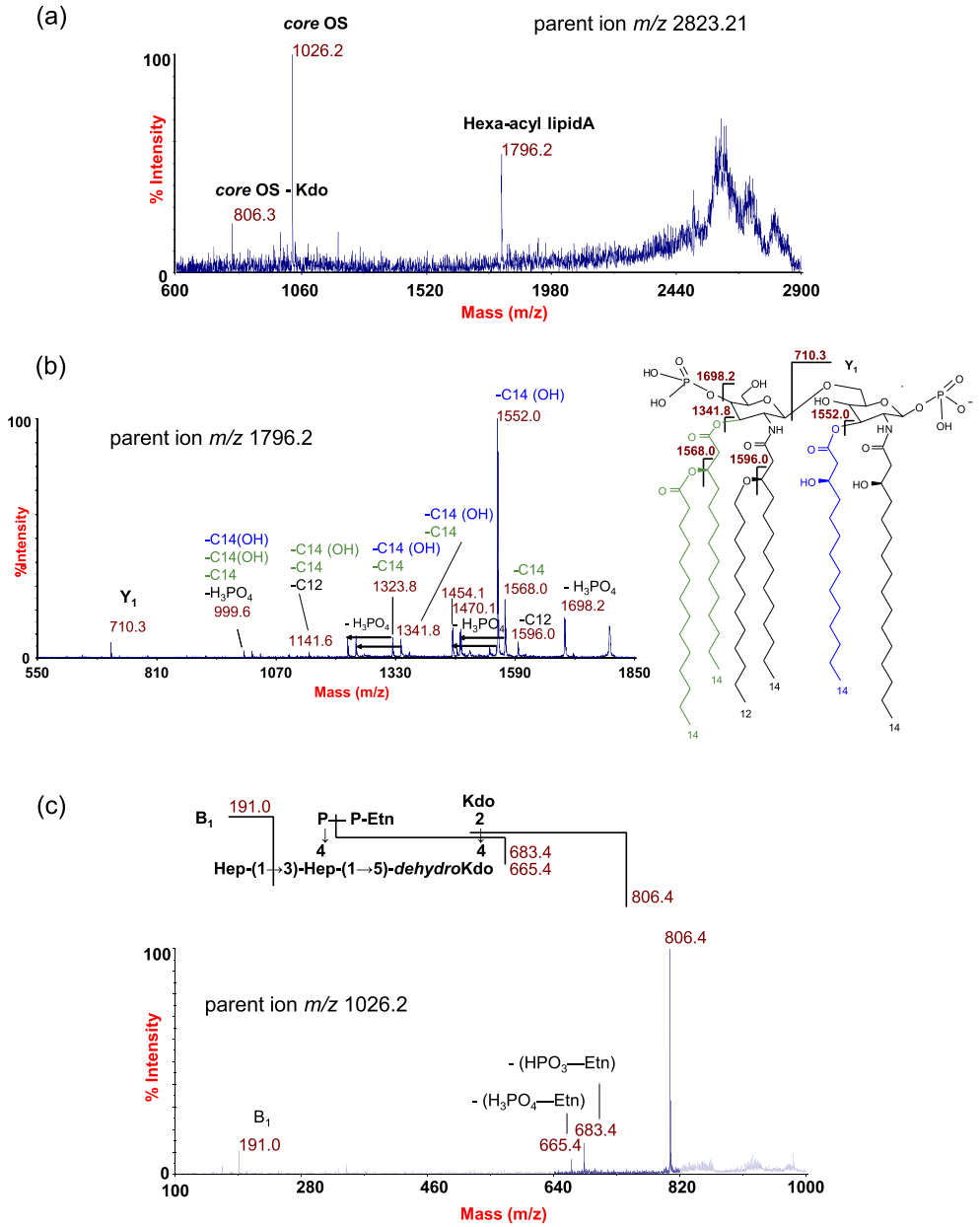

Figure 4. MALDI TOF/TOF analysis of the selected LOS at *m/z* 2823.21 from *Shigella flexneri* M90T *ΔgalU*. (a) Negative-ion tandem mass spectrum of the precursor ion at *m/z* 2823.21 that reveals both lipid A and core OS MMs. This last ion fragment can further lose a Kdo terminal unit giving the peak at *m/z* 806.3. The broad assembly of not well resolved peaks is due to metastable transitions and phosphate groups losses. (b) Negative-ion tandem mass spectrum of species at *m/z* 1796.2, corresponding to the hexa-acyl lipid A structure reported along with its main fragmentations. Ions deriving from to two or more dissociations are also assigned. Different fatty acids are represented with different colors for an easier peaks assignment. (c) Negative-ion tandem mass spectrum of the core OS at *m/z* 1026.2. The base-peak at *m/z* 806.4 originates from terminal Kdo loss. Peaks at *m/z* 683.4 and 665.4 are related to a further loss of phosphoethanolamine. Peak at *m/z* 191.0 corresponds to B_1 ion.

systematically employed for the analysis of complex biomolecules without the necessity of prior chemical degradation, as pivotal structural information can be lost because of chemical treatments that LOS usually undergo in the course of their structural characterization. The in-source regiospecific cleavage of the linkage between the core oligosaccharide and lipid A moiety also provided simultaneous observation of both of these components as ion fragments. The exact MM of the core moieties is highly informative because these species often have a basic heterogeneity due to the presence of chemical groups that are linked in a non-stoichiometric manner. Moreover, the fragmentation spectrum of lipid A provides the location of the fatty acid on the saccharide backbone and details of its structural features.

Here, we have re-examined some LOS structures from three bacteria that belong to the extensively studied genera *Burkholderia*, *Shigella and Yersinia* using this improved technique. Acquisition of high accuracy LOS spectra followed by tandem MS/MS of the lipid A species revealed additional information in two of the cases described.

New perspectives on detection and identification of Gram-negative bacteria with minimal manipulation through the application of MALDI-MS techniques could result from this research. Recently, numerous papers have been published on the rapid

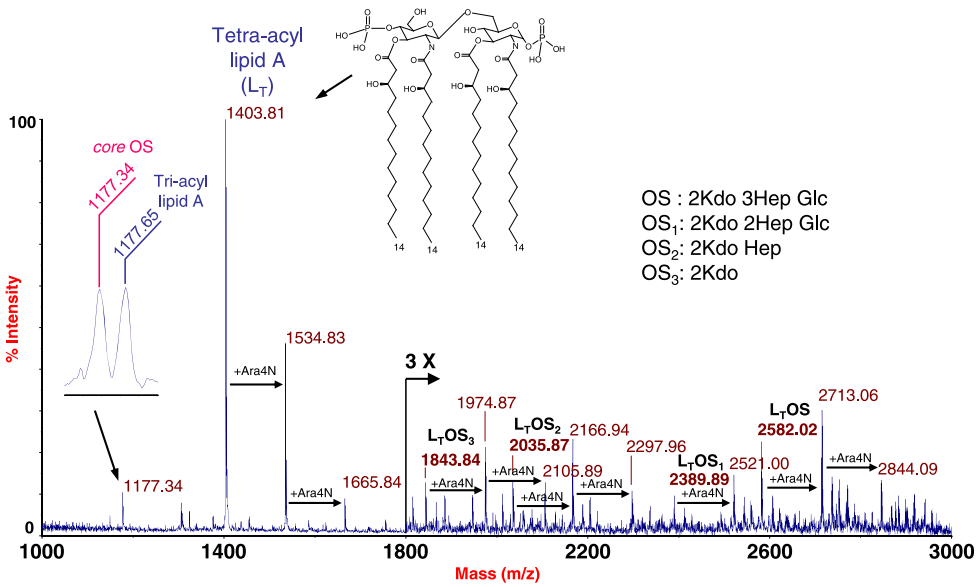

Figure 5. Reflectron MALDI TOF mass spectrum of R-LPS from *Y. pestis* P1680 grown at 37 °C that shows, as main peak, the tetra-acylated lipid A form (L_T) at *m/z* 1403.81. Peak at *m/z* 1177 refers to two different species, as revealed by the expansion of the mass scale (inset): the OS moiety at *m/z* 1177.34 and the tri-acyladed lipidA at *m/z* 1177.65. This spectrum also shows, between *m/z* 1800 and 3000, a heterogeneous mixture of molecular ions which main components are assigned.

identification of bacteria by MALDI MS.[38] Nearly all of these studies use low mass proteins as biomarkers. The presence and relative abundance of these species are highly dependent on bacterial growth, and the validation of this method presents a serious problem. Characterizing bacteria through the MS/MS analysis of their Lipid A component has previously been suggested.[39] The acquisition of reflectron MALDI mass spectra of LOS presents these molecules as potential biomarkers for the rapid recognition of bacteria by MS, which emphasizes the correlation between fingerprinting core OS and lipid A components and chemotaxonomic classification of bacteria.

Acknowledgements

Partial financial support from the Italian Ministry for University and for scientific and technology Research (MIUR-PRIN 2008 and 2009) and from the National Council of Research is gratefully acknowledged. Authors thank prof. M.A. Valvano (University of Western Ontario, Canada) for *Burkholderia* strain and prof. M.L. Bernardini (Università La Sapienza, Roma) for *Shigella* strain.

Supporting Information

Supporting information may be found in the online version of this article.

REFERENCES

[1] A. Preston, R. E. Mandrell, B. W. Gibson, M. A. Apicella. The lipooligosaccharides of pathogenic gram-negative bacteria. *Crit. Rev. Microbiol.* **1996**, *22*, 139.
[2] A. Silipo, C. De Castro, R. Lanzetta, M. Parrilli, A. Molinaro. Lipopolysaccharides. In *Prokaryotic Cell Wall Compounds - Structure and Biochemistry*. (Eds). H. König, H. Claus, A. Varma, Springer: Heidelberg, **2010**, 133–153.
[3] R. Aebersold, M. Mann. Mass spectrometry-based proteomics. *Nature* **2003**, *422*, 198.
[4] S. M. Haslam, S. Julien, J. M. Burchell, C. R. Monk, A. Ceroni, O. A. Garden, A. Dell. Characterizing the glycome of the mammalian immune system. *Immunol. Cell Biol.* **2008**, *86*, 564.
[5] D. S. Cornett, M. L. Reyzer, P. Chaurand, R. M. Caprioli. MALDI imaging mass spectrometry: molecular snapshots of biochemical systems. *Nat. Methods* **2007**, *4*, 828.
[6] B. Lindner. Matrix-assisted laser desorption/ionization time-of-flight mass spectrometry of lipopolysaccharides. In *Methods in Molecular Biology*, 145: Bacterial Toxins: Methods and Protocols. O. Holst (Ed.) Humana Press Inc.: Totowa, **2000**, 311–325.
[7] H. Therisod, V. Labas, M. Caroff. Direct microextraction and analysis of rough-type lipopolysaccharides by combined thin-layer chromatography and MALDI mass spectrometry. *Anal. Chem.* **2001**, *16*, 3804.
[8] B. W. Gibson, J. J. Engstrom, C. M. John, W. Hines, A. M. Falick. Characterization of Bacterial lipooligosaccharides by delayed extraction matrix-assisted laser desorption ionization time-of-flight mass spectrometry. *J. Am. Soc. Mass Spectrom.* **1997**, *8*, 645.
[9] B. Schilling, B. W. Gibson, M. Filiatrault, A. A. Campagnari. Characterization of lipooligosaccharides from *Haemophilus ducreyi* containing polylactosamine repeats. *J. Am. Soc. Mass Spectrom.* **2002**, *13*, 724.
[10] M. Dzieciatkowska, E. K. Schweda, E. R. Moxon J. C. Richards, J. Li. Characterization of intact lipopolysaccharides from the *Haemophilus influenzae* strain RM 118 using electrophoresis-assisted open-tubular liquid chromatography-mass spectrometry. *Electrophoresis* **2008**, *29*, 2171.
[11] Y. A. Knirel, A. N. Kondakova, O. V. Bystrova, B. Lindner, R. Z. Shaikhutdinova, S. V. Dentovskaya, A. P. Anisimov. New features of *Yersinia* lipopolysaccharide structures as revealed by high-resolution electrospray ionization mass spectrometry. *Adv. Sci. Lett.* **2008**, *1*, 192.
[12] L. Sturiale, D. Garozzo, A. Silipo, R. Lanzetta, M. Parrilli, A. Molinaro. New conditions for matrix-assisted laser desorption/ionization mass spectrometry of native bacterial R-type lipopolysaccharides. *Rapid Commun. Mass Spectrom.* **2005**, *19*, 1829.
[13] D. J. Harvey. Analysis of carbohydrates and glycoconjugates by matrix-assisted laser desorption/ionization mass spectrometry: an update for the period 2005–2006. *Mass Spectrom. Rev.* **2011**, *30*, 1.
[14] P. Malvagna, G. Impallomeni, R. Cozzolino, E. Spina, D. Garozzo. New results on matrix-assisted laser desorption/ionization mass spectrometry of widely polydisperse hydrosoluble polymers. *Rapid Commun. Mass Spectrom.* **2002**, *16*, 1599.
[15] A. Silipo, S. Leone, R. Lanzetta, M. Parrilli, L. Sturiale, D. Garozzo, E. L. Nazarenko, R. P. Gorshkova, E. P. Ivanova, N. M. Gorshkova, A.

Molinaro. The complete structure of the lipooligosaccharide from the halophilic bacterium *Pseudoalteromonas issachenkonii* KMM 3549T. *Carbohydr. Res.* **2004**, *339*, 1985.
[16] A. Silipo, S. Leone, A. Molinaro, L. Sturiale, D. Garozzo, E. L. Nazarenko, R. P. Gorshkova, E. P. Ivanova, R. Lanzetta, M. Parrilli. Complete structural elucidation of a novel lipooligosaccharide from the outer membrane of the marine bacterium *Shewanella pacifica*. *Eur. J. Org. Chem.* **2005**, *11*, 2281.
[17] A. Silipo, A. Molinaro, L. Sturiale, J. M. Dow, G. Erbs, R. Lanzetta, M. A. Newman, M. Parrilli. The elicitation of plant innate immunity by lipooligosaccharide of *Xanthomonas campestris*. *J. Biol. Chem.* **2005**, *280*, 33660.
[18] V. Liparoti, A. Molinaro, L. Sturiale, D. Garozzo, E. L. Nazarenko, R. P. Gorshkova, E. P. Ivanova, L. S. Shevcenko, R. Lanzetta, M. Parrilli. Structural analysis of the deep rough lipopolysaccharide from gram negative bacterium *Alteromonas macleodii* ATCC 27126T: the first finding of β-Kdo in the inner core of lipopolysaccharides. *Eur. J. Org. Chem.* **2006**, *20*, 4710.
[19] A. Silipo, A. Molinaro, D. Comegna, L. Sturiale, P. Cescutti, D. Garozzo, R. Lanzetta, M. Parrilli. Full structural characterisation of the lipooligosaccharide of a *Burkholderia pyrrocinia* clinical isolate. *Eur. J. Org. Chem.* **2006**, *21*, 4874.
[20] S. Leone, A. Molinaro, L. Sturiale, D. Garozzo, E. L. Nazarenko, R. P. Gorshkova, E. P. Ivanova, L. S. Shevchenko, R. Lanzetta, M. Parrilli. The outer membrane of the marine gram-negative bacterium *Alteromonas addita* is composed of a very short-chain lipopolysaccharide with a high negative charge density. *Eur. J. Org. Chem.* **2007**, *7*, 1113.
[21] A. Silipo, A. Molinaro, T. Ieranò, A. De Soyza, L. Sturiale, D. Garozzo, C. Aldridge, P. A. Corris, C. M. Khan, R. Lanzetta, M. Parrilli. The complete structure and pro-inflammatory activity of the lipooligosaccharide of the highly epidemic and virulent gram-negative bacterium *Burkholderia cenocepacia* ET-12 (strain J2315). *Chem.–Eur. J.* **2007**, *13*, 3501.
[22] T. Ieranò, A. Silipo, L. Sturiale, D. Garozzo, H. Brookes, C. M. Khan, C. Bryant, F. K. Gould, P. A. Corris, R. Lanzetta, M. Parrilli, A. De Soyza, A. Molinaro. The structure and proinflammatory activity of the lipopolysaccharide from *Burkholderia multivorans* and the differences between clonal strains colonizing pre and posttransplanted lungs. *Glycobiology* **2008**, *18*, 871.
[23] C. M. John, M. Liu, G. A. Jarvis. Profiles of structural heterogeneity in native lipooligosaccharides of *Neisseria* and cytokine induction. *J. Lipid Res.* **2009**, *50*, 424.
[24] C. M. John, M. Liu, G. A. Jarvis. Natural phosphoryl and acyl variants of lipid A from *Neisseria meningitidis* strain 89I differentially induce tumor necrosis factor-alpha in human monocytes. *J. Biol. Chem.* **2009**, *284*, 21515.
[25] T. Ieranò, A. Silipo, L. Sturiale, D. Garozzo, P. Corris, J. Perry, R. Lanzetta, M. Parrilli, A. De Soyza, A. Molinaro. Structural elucidation of a novel *B. cenocepacia* ET-12 lipooligosaccharide isolated from a cystic fibrosis patient after lung transplantation. *Eur. J. Org. Chem.* **2010**, *7*, 1299.
[26] B. Domon, C. E. Costello. A systematic nomenclature for carbohydrate fragmentations in FAB-MS/MS spectra of glycoconjugates. *Glycoconj. J.* **1988**, *5*, 397.
[27] C. De Castro, M. Parrilli, O. Holst, A. Molinaro. Microbe-associated molecular patterns in innate immunity: Extraction and chemical analysis of gram-negative bacterial lipopolysaccharides. *Methods Enzymol.* **2010**, *480*, 89.
[28] X. Ortega, A. Silipo, M. S. Saldías, C. C. Bates, A. Molinaro, M. A. Valvano. Biosynthesis and structure of the *Burkholderia cenocepacia* K56-2 lipopolysaccharide core oligosaccharide: truncation of the core oligosaccharide leads to increased binding and sensitivity to polymyxin B. *J. Biol. Chem.* **2009**, *284*, 21738.
[29] B. W. Gibson, J. J. Engstrom, W. Hines, H. P. Wight, A. Falick. MALDI Post Source Decay and CID analysis of bacterial glycolipids. Proc. of 45th ASMS Conference on Mass Spectrometry and Allied Topics. **1997**, 1129.
[30] S. Chan, V. N. Reinhold. Detailed structural characterization of lipid A: electrospray ionization coupled with tandem mass spectrometry. *Anal. Biochem.* **1994**, *218*, 63.
[31] I. A. Kaltashov, V. Doroshenko, R. J. Cotter, K. Takayama, N. Qureshi. Confirmation of the structure of lipid A derived from the lipopolysaccharide of *Rhodobacter sphaeroides* by a combination of MALDI, LSIMS, and tandem mass spectrometry. *Anal. Chem.* **1997**, *69*, 2317.
[32] A. Silipo, C. De Castro, R. Lanzetta, A. Molinaro, M. Parrilli, G. Vago, L. Sturiale, A. Messina, D. Garozzo. Structural characterizations of lipids A by MS/MS of doubly charged ions on a hybrid linear ion trap/orbitrap mass spectrometer. *J. Mass Spectrom.* **2008**, *43*, 478.
[33] S. W. Montminy, N. Khan, S. McGrath, M. J. Walkowicz, F. Sharp, J. E. Conlon, K. Fukase, S. Kusumoto, C. Sweet, K. Miyake, S. Akira, R. J. Cotter, J. D. Goguen, E. Lien. Virulence factors of *Yersinia pestis* are overcome by a strong lipopolysaccharide response. *Nat. Immunol.* **2006**, *7*, 1066.
[34] R. C. Murphy, C. R. Raetz, C. M. Reynolds, R. M. Barkley. Mass spectrometry advances in lipidomica: collision-induced decomposition of Kdo_2-lipid A. *Prostaglandins Other Lipid Mediat.* **2005**, *77*, 131.
[35] B. Schilling, M. K. McLendon, N. J. Phillips, M. A. Apicella, B. W. Gibson. Characterization of lipid A acylation patterns in *Francisella tularensis*, *Francisella novicida*, and *Francisella philomiragia* using multiple-stage mass spectrometry and matrix-assisted laser desorption/ionization on an intermediate vacuum source linear ion trap. *Anal. Chem.* **2007**, *79*, 1034.
[36] A. Molinaro, A. Silipo, C. De Castro, L. Sturiale, G. Nigro, D. Garozzo, M. L. Bernardini, R. Lanzetta, M. Parrilli. Full structural characterization of *Shigella flexneri* M90T serotype 5 wild-type R-LPS and its *ΔgalU* mutant: glycine residue location in the inner core of the lipopolysaccharide. *Glycobiology* **2008**, *18*, 260.
[37] K. Kawahara, H. Tsukano, H. Watanabe, B. Lindner, M. Matsuura. Modification of the structure and activity of lipid A in *Yersinia Pestis* lipopolysaccharide by growth temperature. *Infect. Immun.* **2002**, *70*, 4092.
[38] Y. A. Knirel, B. Lindner, E. V. Vinogradov, N. A. Kocharova, S. N. Senchenkova, R. Z. Shaikhutdinova, S. V. Dentovskaya, N. K. Fursova, I. V. Bakhteeva, G. M. Titareva, S. V. Balakhonov, O. Holst, T. A. Gremyakova, G. B. Pier, A. P. Anisimov. Temperature-dependent variations and intraspecies diversity of the structure of the lipopolysaccharide of *Yersinia pestis*. *Biochemistry* **2005**, *44*, 1731.
[39] Y. A. Knirel, B. Lindner, E. Vinogradov, R. Z. Shaikhutdinova, S. N. Senchenkova, N. A. Kocharova, O. Holst, G. B. Pier, A. P. Anisimov. Cold temperature-induced modifications to the composition and structure of the lipopolysaccharide of *Yersinia pestis*. *Carbohydr. Res.* **2005**, *340*, 1625.
[40] A. Kondakov, B. Lindner. Structural characterization of complex bacterial glycolipids by Fourier transform mass spectrometry. *Eur J Mass Spectrom.* **2005**, *11*, 535.
[41] S. Sauer, M. Kliem. Mass spectrometry tools for the classification and identification of bacteria. *Nat. Rev. Microbiol.* **2010**, *8*, 74.
[42] I. A. Kaltashov, N. Qureshi, T. Odegaard, C. R. H. Raetz, R. J. Cotter. Fast and sensitive characterization of lipid A: A potential application to bacteria identification. *Adv Mass Spectrom* **1998**, 14.